EPJ Photovoltaics **15**, 7 (2024)

https://doi.org/10.1051/epjpv/2024001

Available online at:
www.epj-pv.org

Special Issue on 'EU PVSEC 2023: State of the Art and Developments in Photovoltaics', edited by Robert Kenny and João Serra

ORIGINAL ARTICLE OPEN ACCESS

The effect of partial shading on the reliability of photovoltaic modules in the built-environment

Ebrar Özkalay[1,2,*], Flavio Valoti[1], Mauro Caccivio[1], Alessandro Virtuani[2,3], Gabi Friesen[1], and Christophe Ballif[2,3]

[1] University of Applied Sciences and Arts of Southern Switzerland (SUPSI-PVLab), Via Flora Ruchat-Roncati 15, 6850 Mendrisio, Switzerland
[2] École Polytechnique Fédérale de Lausanne (EPFL), Institute of Electrical and Micro Engineering (IEM), Photovoltaics and Thin-Film Electronics Laboratory, Rue de la Maladière 71b, 2002 Neuchâtel, Switzerland
[3] Swiss Centre for Electronics and Microtechnology (CSEM), Sustainable Energy Center, Rue de Jaquet-Droz 1, 2002 Neuchâtel, Switzerland

Received: 3 October 2023 / Accepted: 8 January 2024

Abstract. Residential photovoltaic systems often experience partial shading from chimneys, trees or other structures, which can induce hot-spots in the modules. If the temperature and frequency of these hot-spots are high, the module's reliability and safety may be at risk. IEC 61215-2:2021 hot-spot endurance test is utilized to evaluate the materials' ability to withstand partial shading. Since modules in residential systems can be subjected to higher temperatures than those in the open field, IEC TS 63126:2020 recommends adjusting the module temperature for the hot-spot endurance test according to the module's operating temperature. This study tested the hot-spot endurance of PERC, IBC and HJT modules under standard (55 °C) and more severe (75 °C, Level 2 condition in IEC TS 63126:2020) test conditions, as well as outdoor accelerated-ageing tests were performed with shadow masks. The results demonstrated that irrespective of environmental conditions, hot-spots can form at lower temperatures, with more shading-tolerant cells (i.e., cells with lower breakdown voltage) or with shorter strings. We also show that it is possible to shorten the effort- and time-consuming hot-spot endurance test described in the standard and obtain similar results. In addition, the hot-spot endurance test for residential PV systems was evaluated in terms of module temperatures and duration. In this respect, we propose to increase the testing temperatures of the hot-spot endurance testing for modules operating at high temperatures in IEC TS 63126:2020.

Keywords: Shadow / partial shading / hot-spot endurance test / residential PV / BIPV / reliability

1 Introduction

The operating conditions of photovoltaic (PV) modules in built environments are more susceptible to additional stressors, such as shading and elevated temperatures, compared to those designed for large-scale installations in moderate climates [1–3]. Temperature-induced degradation has been examined in some studies [4,5], and the International Electrotechnical Commission (IEC) has proposed modifications to typical module qualification and safety tests (i.e. IEC 61215-2:2021 [6], and IEC 61730-2:2023 [7]) for modules operating at high temperatures in IEC TS 63126:2020 [8]. However, the shadow-induced degradation of PV modules in residential systems has received limited attention. Unlike large PV fields, where large areas generally ensure optimal operating conditions without obstacles, the presence of structures such as chimneys, nearby buildings, or trees in the built environment can create challenges in maximizing the production and reliability of PV modules in the presence of persistent shadows. The presence of a partial shadow can induce a hot-spot that is significantly hotter than the other parts of the module and can reach temperatures as high as 130−150 °C (or higher). The occurrence of hot-spots may prospectively lead to the generation of other failure modes, such as discolouration, interconnection failures and cell cracks, delamination and loss of electrical insulation. Mitigation measures are therefore being introduced by the manufacturers. The key questions are (1) whether these mitigation measures are sufficient for residential PV components, and (2) whether the existing hot-spot endurance test methods are representative of the residential PV conditions.

* e-mail: ebrar.ozkalay@supsi.ch

In this study, the term "hot-spot" was used as defined by the IEC. That is, a hot-spot occurs when the operating current of the module exceeds the reduced short-circuit current (I_{sc}) of a shaded or faulty cell or group of cells. In contrast, the International Energy Agency (IEA) states that the hot-spot can be caused by (i) reverse bias and junction breakdown of a solar cell, (ii) damaged cell, or (iii) damaged metallisation [9]. The reason why the term "hot-spot" is defined differently is explained in [10].

1.1 Hot-spot phenomena

When a module is exposed to partial shade, a bypass diode (BPD) can be activated depending on the dynamic maximum power point of the module. In the event of an activated diode, BPD heats up as the current difference between the unshaded string(s) and the partially shaded cell flows through the activated BPD (Fig. 1). In addition, the decrease in photocurrent of the shaded cell causes a disparity in operating points between the series-connected cells, which subsequently forces the shaded cell to operate at a negative voltage. The reverse characteristics of the shaded cell (i.e., shunt resistance and breakdown voltage) are largely responsible for the robust reverse bias operation of the cell and module performance in partial shade [11,12]. Conventional multicrystalline silicon solar cells typically have three reverse bias breakdown mechanisms, known as early breakdown (−4V to −9V), soft breakdown (−9V to −13V), and hard breakdown (beyond −13V) [13,14]. Conventional monocrystalline silicon solar cells exhibit a relatively linear relationship between the reverse current and voltage at low reverse bias voltages [15]. The most important mechanism for junction breakdown in monocrystalline silicon solar cells is avalanche breakdown [16,17]. This breakdown occurs at reverse bias voltages below −20V for PERC cells, the most common type of mass-produced solar cell [10]. Junction breakdown occurs at the weakest point in the cell area. Under reverse bias operation, the leakage current distribution may not be uniform, and one of them may develop into a hot-spot [18,19]. The partial shading of a solar cell can result in higher temperatures in the illuminated portion of the cell compared to the shaded portion [20]. This is because the illuminated portion of the cell absorbs more light, leading to a higher operating temperature than for the shaded portion. As a result, the solar cell, module materials (i.e., glass, encapsulant, and metallization), and diode may be subject to high thermal stress. While other parts of the module typically operate at temperatures of 50−70 °C, a hot-spot can cause heating above these temperatures, reaching temperatures of 130−150 °C (or higher).

1.2 Hot-spot mitigation and testing

Degradation caused by hot-spot may endanger the reliability and durability of solar panels, for this reason manufacturers take measures to mitigate its impact. These include cell sorting into bins based on cell's current output, screening individual cells for low shunt resistance, and using BPDs to redirect current flow around problematic or shaded cells. Produced PV cells are tested for power (and current) output and grouped with other cells of similar output. Modules are then constructed from cells within the same bin to minimize mismatch losses between cells in series [21]. In addition, most manufacturers also discard cells that are deemed susceptible to hot-spot (low shunt resistant cells) to prevent this degradation from occurring [22,23]. Most importantly, manufacturers include BPDs in their PV modules to prevent hot-spot formation and mitigate its harmful effects. However, BPDs only reduce the negative impacts of hot-spots and do not entirely eliminate them. Although a BPD reduces the power losses that can be caused by shadows [24], shadow events that have become a daily routine still pose severe performance losses and safety risks. These risks are often overlooked during the design and material selection of PV modules. Moreover, a growing variety of PV modules that are advertised as shade-resistant may be found on the market due to an improved understanding of the effects of shading events on the overall output power. However, shade resistance is poorly defined and there is no reliable way to compare different PV products. In addition, minimizing yield loss is generally the primary focus of shade-resistant modules [25,26]. However, improved reliability is often neglected or not considered. The hot-spot endurance (HS) test (IEC 61215-2:2021) assesses the ability of a module to resist local point heating at a module temperature of 55±15 °C under partial shading. This test simulates a worst-case hot-spot scenario to evaluate the performance of the module and its ability to withstand hot-spotting without damage or degradation. The execution of this test is now even more important due to the increasing occurrence of hot-spot on new module technologies [27] and the fact that they can further accelerate other failure mechanisms that cause safety issues (e.g., loss of electrical insulation). The HS test in its present version requires a maximum of 5 h to perform under a light source. However, considering that residential PV systems can be subjected to frequent shadow events, it is not surprising that the total time spent in the presence of a hot-spot can largely exceed 5 h over the lifetime of a residential PV system. In the case of persistent shading, this thermal stress will always affect the same area and diode (strongly soliciting BPD). For these reasons, the module may eventually lose its performance or the diode may lose its functionality. Bypass diodes can fail in two modes: short-circuit and open-circuit. (a) In short-circuit failure mode, the string of cells connected in parallel is short-circuited, resulting in power loss depending on the electrical layout. For example, when a BPD is shorted, typically one-third of the power of a conventional module is lost depending on the electrical layout. (b) In open-circuit failure mode, the BPD cannot conduct any current and has no impact on the power output of the PV module. This is similar to a string of solar cells without a BPD. However, if a BPD fails in the open-circuit mode, the protection provided by the BPD is lost, and hot-spot can occur very quickly in the presence of shade [28]. Furthermore, fire risks can occur in urban areas under the specific conditions (e.g., full roof integration). Therefore, choosing a PV module suitable for residential PV systems and testing these modules under representative conditions is crucial.

2 Experimental approach

In this study, the reliability of modules due to repeated partial shading in a residential environment was analysed by performing HS tests under standard conditions (IEC 61215-2:2021) and under extended test conditions (specifically at higher module temperatures according to IEC TS 63126:2020) and duration. In parallel to indoor testing, the HS tests were complemented by performing outdoor accelerated-ageing monitoring for over one year of modules covered with shadow masks. The hot-spot temperatures obtained in the HS tests were expected to be higher than those observed in the outdoor tests – during realistic operating conditions – because the HS tests were designed to simulate the worst-case scenarios. The HS and outdoor accelerated-ageing tests were carried out on different module technologies and designs (i.e., Passivated Emitter and Rear Contact (PERC), Interdigitated Back Contact (IBC), Heterojunction Technology (HJT), and modules with shorter cell-string, etc.) to investigate the behaviour, operating conditions, and tolerance of different PV module technologies in the case of partial shading. Meanwhile, we also investigated the sufficiency of the indoor hot-spot endurance test (IEC 61215-2:2021) for residential PV systems, taking into account higher operating temperatures and more frequent partial shading events with respect to field-deployed PV systems. In addition, one of our aims was to stress beyond standard test conditions to address the operation of modules in building-integrated PV (BIPV) conditions.

2.1 Hot-spot endurance test (indoor)

The standard procedure of the IEC 61215-2:2021 HS test is divided into three steps. The initial steps, which are cell selection (Step 1) and determination of worst-case shadow conditions of the selected cells (Step 2), are the most effort- and time-consuming parts of the test. The three steps are as follows [22,29]:

Step 1) In order to select the hot-spot sensitive cells, each cell of the module is completely shaded, and a current-voltage characteristic (IV curve) is measured for each cell (Fig. 2a). Then, four cells are selected; (i) one cell with the lowest shunt resistance adjacent to the edge of the module, (ii-iii) two cells with the lowest shunt resistance cells, and (iv) one cell with the highest shunt resistance.

Step 2) In the next step, if the cell circuit is not accessible, one of the options to determine the worst-case shading of the selected cells is partially shadowing each of these four cells in turn and performing IV measurements. The worst-case shading occurs when the current through the shaded cell (the point at which the BPD turns on, $I_{sc,shaded\ cell}$) coincides with the maximum power current of the unshaded module ($I_{mpp,unshaded}$) (Fig. 2b).

Step 3) The final step of the HS test is to expose the module under short circuit condition to steady state irradiance ($1000\pm100\,W/m^2$) for at least 1 h while shading the four selected cells individually one at a time. According to IEC 61215-2:2021, if the temperature of the shaded cell continues to increase after 1 h of exposure, the experiment continues for a total of up to 5 h. However, since in the built environment it is likely to have persistent shading events extending for more than 5 h, we extended the HS tests duration up to 10 h.

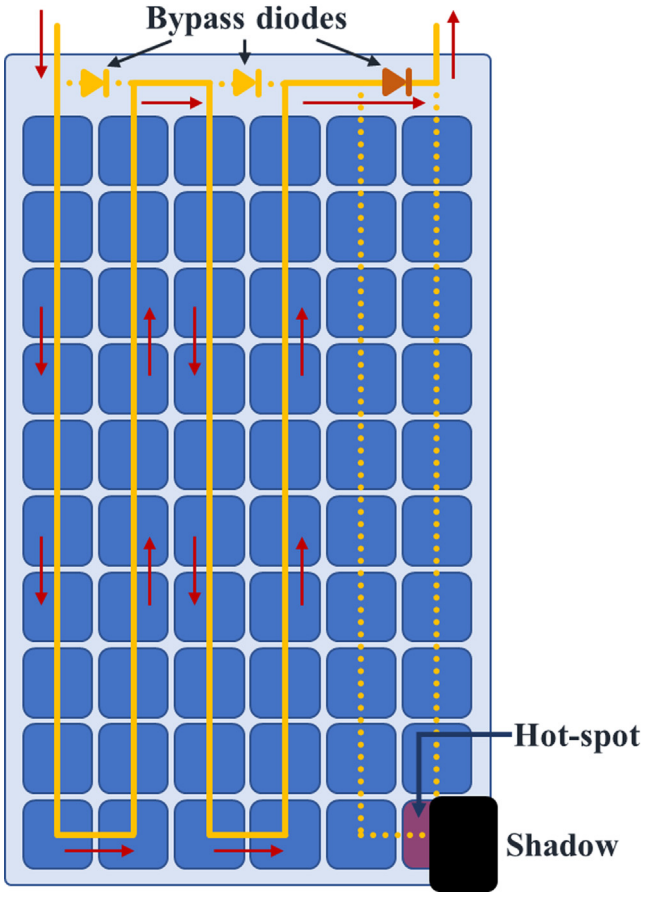

Fig. 1. Simple schematic of a conventional 60-cell PV module with three bypass diodes (3 strings in series) under partial shading conditions of a cell with an activated bypass diode. Hotter bypass diode and cell are indicated by using different colours. Red arrows indicate current flow.

To shorten this effortful HS test, we tried shortening the steps of cell selection (Step 1) and determining the worst-case shadow (Step 2) as described below:

Step 1) For cell selection, since cells are usually screened for low shunt resistance, and the susceptible ones are discarded, we tried to randomly select four cells instead of performing IV measurements for each cell of a module as in the standard. In this study, depending on the number of cells in the modules, such cell selection saves between 30 and 120 IV curve measurements per module (corresponding to a time savings of between 30 and 120 min).

Step 2) For the worst-case shadow determination, we assumed that partial shading affects the shaded cell's short circuit current ($I_{sc,shaded\ cell}$) as follows [30].

$$I_{sc,shaded\ cell} = (1 - R) \times I_{sc,unshaded} \quad (1)$$

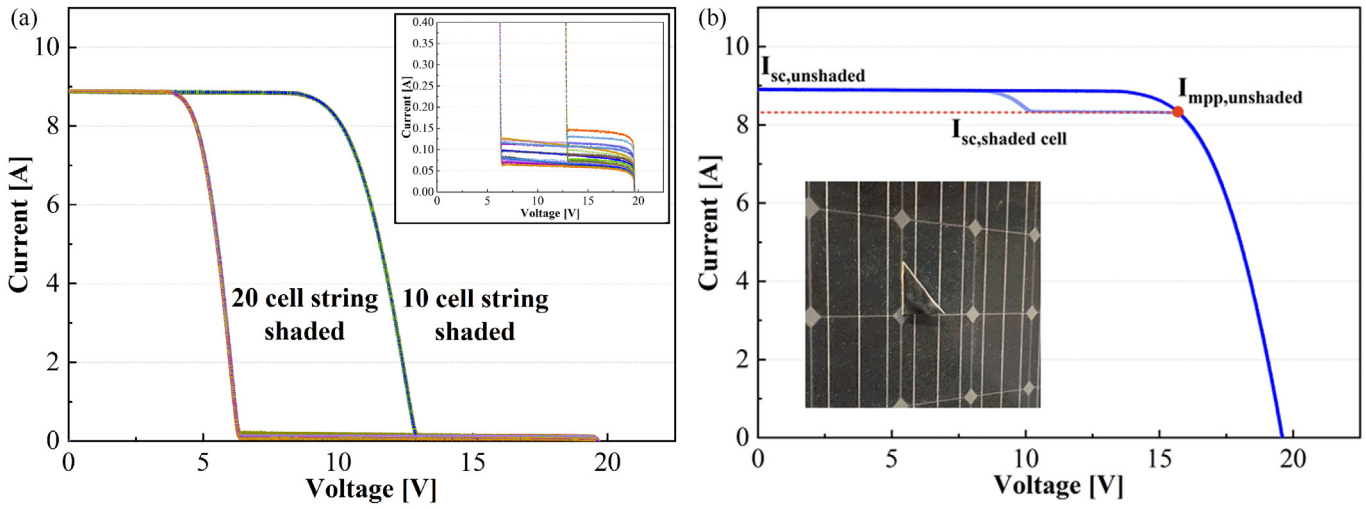

Fig. 2. (a) IV characteristics of the PERC cell-based module with each cell totally shaded. (b) IV characteristics of the PERC cell-based module with a selected cell shaded in the worst-case.

with the shading rate R as the ratio of shaded area to full cell area. Since the worst-case shadow occurs when the shaded cell's short circuit current ($I_{sc,shaded\ cell}$) coincides with the maximum power point current of the unshaded module ($I_{mpp,unshaded}$) the worst-case shadow rate (R_{worst}) an be determined using the following formula.

$$R_{worst} = \frac{I_{sc,unshaded} - I_{mpp,unshaded}}{I_{sc,unshaded}} \quad (2)$$

where $I_{sc,unshaded}$ is the short-circuit current of the unshaded module. The advantage of this approach is that it eliminates the need to experimentally determine the worst-case shadow ratio by preparing different shadow masks and performing IV measurements with these masks separately for each of the four selected cells. The formula for calculating the worst-case shadow rate is only applicable when only one BPD is connected to a cell string, as is typically done in conventional PV modules. In cases where cells have an extremely low shunt resistance (high leakage current), it is necessary to include a correction term in formula (2). Without this correction, the shading ratio will be underestimated, the degree of which depends on the level of the shunt resistance.

Step 3) The final step, which is exposing the module under short circuit condition to steady state irradiance ($1000\pm100\,W/m^2$) for at least 1 h while shading the four selected cells individually one at time, remained same.

Furthermore, the technical specification IEC TS 63126:2020 [8] describes the changes in the test conditions of some typical reliability and safety tests in IEC 61215-2:2021 and IEC 61730-2:2023 needed to take into account modules operating at high temperatures (e.g., residential PV, building attached PV, BIPV and hot climates). IEC TS 63126:2020 suggests using the 98th percentile of operating module temperature (T_{98}) to assess whether a module is operating at high temperatures. The temperature represented by T_{98} is significantly higher than 98% of the remaining temperatures and is met or exceeded only 2% of the time. Depending on the T_{98}, equivalent to 175.2 h/year, more severe test conditions are recommended for several qualification and safety tests (Level 1 test conditions for $70\,°C < T_{98} \leq 80\,°C$ and Level 2 test conditions for $80\,°C < T_{98} \leq 90\,°C$) [31]. The HS test is one of the tests whose testing conditions vary according to T_{98}. The suggested module temperatures (T_{mod}) during the HS test are $60\pm10\,°C$ and $70\pm10\,°C$ at Level 1 and at Level 2, respectively (see in Tab. 3). These proposed module temperature values are 10 °C and 20 °C higher than the module temperature in the standard HS test in effect at the year of publication (2020). It should be noted that when IEC TS 63126:2020 was published, IEC 61215-2:2016 was still in force, and the temperature for the standard HS test was $50\pm10\,°C$. In IEC 61215-2:2021, this module temperature has been updated to $55\pm15\,°C$. For this reason, we set the module temperature 20 °C higher than the current IEC 61215-2:2021 when performing the HS test under Level 2 conditions of IEC TS 63126:2020 ($75\pm15\,°C$).

2.2 Outdoor accelerated-ageing

The same module technologies tested indoors were also monitored outdoors in various BIPV configurations (see Tab. 1) under shaded and unshaded conditions. The test stand at SUPSI in Mendrisio, Switzerland (45.87°N, 8.98°E), which is a Cfb Köppen–Geiger climate zone (temperate and humid climate with warm summers) [32], is operational since the beginning of July 2022. The modules on the test stands were installed in BIPV-partially-ventilated and BIPV-insulated configurations (Fig. 3). In the BIPV-partially-ventilated configuration, a ventilation chamber between the module and the insulation layer provides partial ventilation of the rear of the module. In the BIPV-insulated configuration, there is no air gap between the module and the insulation layer (no ventilation).

Table 1. Details on the modules (and cell technology) used and the indoor and outdoor test conditions.

Module technology	Indoor hot-spot endurance tests		Outdoor tests (monitoring)	
	IEC 61215-2:2021 (55 °C, 5 h) + *5 h**	IEC TS 63126:2020 Level 2 (75 °C**, 5 h) + *5 h**	BIPV***	BIPV*** & shadow mask
1 – PERC – Half-Cell (20 cells/diode)	1	1	1 (Insulated)	1 (Insulated)
2 – IBC – Full-Cell (104 cells, 3 dio des)	1	1	1 (Insulated)	1 (Insulated)
3 – HJT – Half-Cell (20 cells/diode)	1	1	1 (Insulated)	1 (Insulated)
4 – PERC – Full-cell (10 cells/diode + 20 cells/diode)	1	–	1 (Partially Ventilated)	1 (Partially Ventilated)

PERC: Passivated Emitter and Rear Contact, IBC: Interdigitated Back Contact, HJT: Heterojunction technology
* Extended hot-spot test with a total duration of 10 h.
** As stated in the text, the module temperature was considered to be 75 °C instead of 70 °C.
*** The BIPV mounting configuration are indicated for each module technology.

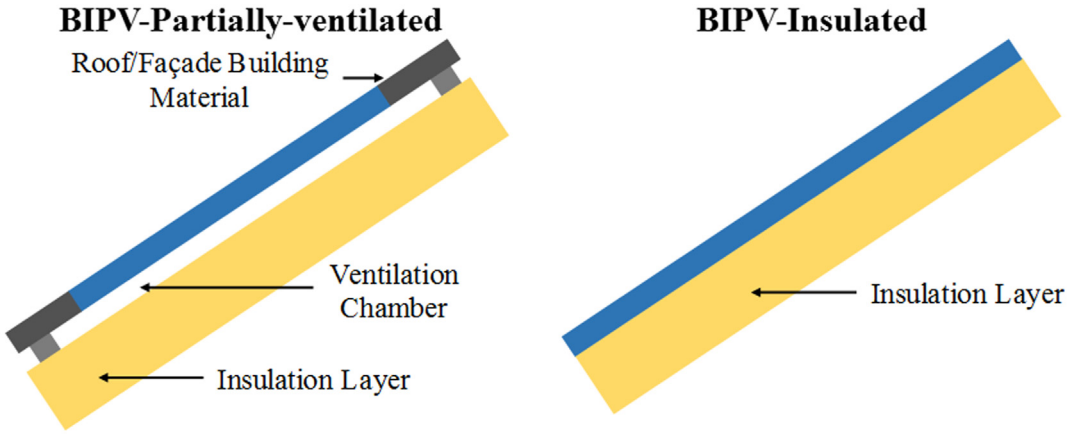

Fig. 3. Simplified summary of the installation configurations for the BIPV test stands.

For the outdoor exposed modules, shadow masks were used to accelerate the degradation that may result from recurring partial shading (Fig. 4a). The shadow masks (36% transmittance) were placed on the long edge of the modules to represent repetitive shading that can occur in residential PV systems due to, e.g., a nearby building or self-shading. The masks covered an area sufficient to activate the BPD connected in parallel with the shaded string. Thus, thermal stress was created on the partially shaded cell (reverse bias heating) and the BPD (which was constantly heating up during day time due to its activation). The widths of the masks were determined in order to have a 10±5% difference between the global P_{mpp} (at low voltage) and local P_{mpp} (at high voltage) in IV measurements at standard test conditions (STC) (Fig. 4b). Although very high temperatures (e.g., 200 °C) could be obtained with a localized shade in a single cell (simulating a bird dropping, etc.), the long edge shade was preferred because it may better represent residential PV systems.

During the outdoor monitoring, each module's maximum power (P_{mpp}) and IV curves are individually monitored at 1-min intervals. The modules were kept at global maximum power point between the IV measurements. The global plane of array irradiance (G_{POA}) is measured by a well-maintained and recalibrated secondary standard pyranometer, and the rear-side module temperature is measured by Pt100 at 1-min intervals. In addition, temperature sensors were placed behind the illuminated part of a partially shaded cell and inside the junction boxes (not directly on the diodes, as the junction boxes are potted), in which a single active BPD is present due to the presence shadow mask. After 13 months of monitoring, indoor tests, namely visual inspection (VI), insulation (INS), wet-leakage (WL), electroluminescence (EL), performance measurement (P_{mpp}, I_{sc}, V_{oc}, FF) at STC and diode functionality test were performed on the outdoor exposed modules in order to assess changes in the device performance.

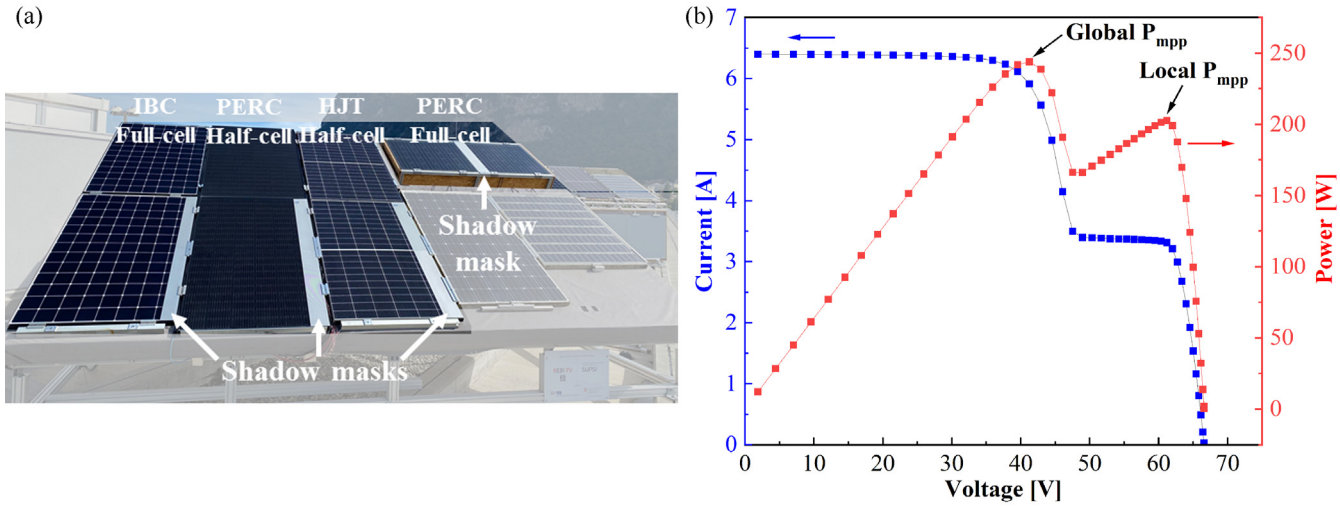

Fig. 4. (a) The outdoor test stand with shaded and unshaded IBC – Full-cell, PERC – Half-cell, HJT – Half-cell and PERC – Full-cell modules. (b) The indoor-measured IV curve of IBC – Full-cell at STC with the selected shadow mask (bypass diode is active, and 13% difference between Global P_{mpp} and Local P_{mpp}).

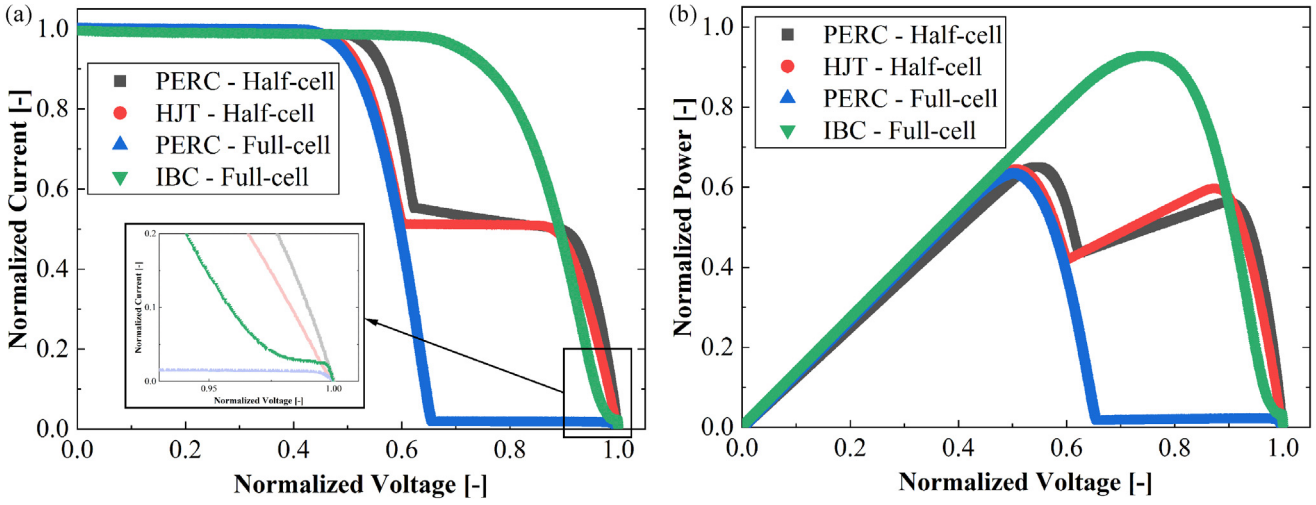

Fig. 5. Normalized (a) current-voltage (IV) and (b) power-voltage curves of PERC – Half-cell, IBC – Full-cell, HJT – Half-cell and PERC – Full-cell modules with completely shaded cell. Power, current, and voltage normalizations were made using unshaded measurements of the same modules.

2.3 Test program and samples

Module technologies with different cell technologies, string lengths and interconnection schemes were chosen for this study. As shown in Table 1, the HS tests were performed in both standard (IEC 61215-2:2021, $T_{mod} = 55\,°C$), extended conditions (IEC TS 63126:2020, $T_{mod}=75\,°C$) and durations ($5\,h + 5\,h$) on PERC – Half-cell, IBC – Full-cell and HJT – Half-cell module technologies. For PERC – Full-cell module, the HS tests were performed only in standard condition (IEC 61215-2:2021, $T_{mod}=55\,°C$) and extended duration ($5\,h + 5\,h$). The PERC – Full-cell module has an asymmetric electrical layout with 2 strings of 10 and 20 cells each. All module types underwent accelerated-ageing in the field for over 1 year.

3 Results

3.1 Hot-spot endurance tests (indoor)

3.1.1 Cell selection

Figure 5 shows normalized current-voltage and power-voltage curves for each tested module technology with one cell completely shaded. As described above, four cells were selected for each module in accordance with IEC 61215-2:2021. For the PERC – Full-cell module, because two strings are connected in series (no parallel connected strings), shading of a cell resulted in a complete loss of current from the string to which the shaded cell is connected. The Half-cell modules have parallel strings. While the current from the string to which the shaded cell

Table 2. The worst-case shading rates of the four selected cells for each module technology determined by following the IEC 61215-2:2021 and shortened procedures.

Module technology	Worst-case shading rates of Cell-1, Cell-2, Cell-3 and Cell-4	
	IEC 61215-2:2021 procedure	Shortened IEC 61215-2:2021 procedure
PERC Half-Cell	9%	10.5%
	9%	9.9%
IBC Full-Cell	100%	100%
	100%	100%
HJT Half-Cell	14%	11.8%
	14%	12.3%
PERC Full-cell	8%, 8%, 10% and 15%	11.9%

is connected is completely lost, the parallel string can supply current at half of the short-circuit current. Complete or partial shading of a cell is sufficient to activate the diode in the PERC and HJT modules in this work, however this is not the case in the IBC module. In IBC solar cells, the p+ and n+ regions are designed to be in direct contact with each other, resulting in the formation of a Zener diode that functions as a built-in BPD and significantly lowers the breakdown voltage (>−5V) of the cell [33] (Fig. 5a). The contact between the two highly doped regions allows carriers to tunnel directly from one band to another (uniform reverse current), leading to uniform heating of the cell as opposed to the formation of local hot-spots and irreversible shunting in standard cells [34].

3.1.2 Worst-case shading rates

Table 2 shows the worst-case shading rates of the modules, which were determined by following the standard and shortened procedures obtained with equations (1) and (2). There is no significant difference between the worst-case shading rates from the two procedures. However, the critical factor is the hot-spot temperature under a continuous light source. Hot-spot temperatures comparable to the standard procedure must be produced to validate the shortened procedure.

As previously explained, completely shading a cell (100%) in IBC modules does not activate the diode. IEC 61215-2:2021 states that the worst-case shading in such a situation is complete shading of a cell. Therefore, a complete shading of a cell is required for HS test of IBC modules. In addition, although all modules have the same worst-case shading rate for the selected cells, the PERC full-cell module has different worst-case shading ratios for its cells. This is due to the fact that this module has been monitored outdoors for over four years, and the mismatch between the cells naturally increases over time. All other modules were exposed outdoors for the first time.

3.1.3 Hot-spot temperatures (indoor)

Figures 6a and 6b show the module and hot-spot temperatures of PERC − Half-cell, IBC − Full-cell and HJT − Half-cell modules from the HS tests at 55 °C and 75 °C module temperatures, respectively. IBC is the module technology with the lowest hot-spot temperatures in the HS test performed at both temperatures. In the 75 °C test, the hot-spot temperature barely exceeded 105 °C. Considering the effect of thermal stress on the degradation of polymeric materials, this causes less stress than for the other module types. The highest hot-spot temperature was seen in the HJT module technology with temperatures rising to 180−190 °C in the HS test at 75 °C module temperature. The difference between the hot-spot and module temperatures of the IBC and HJT technologies remained the same when the module temperature of the HS test was increased from 55 °C to 75 °C. The temperature differences for the IBC and HJT modules are 10−20 °C and 85−100 °C, respectively. Unlike in the other modules, the temperature difference for the PERC − Half-cell module is significantly different in the HS tests at different module temperatures. In the 55 °C test, the hot-spot temperature of the PERC module was 80−110 °C. When the HS test was performed at a module temperature of 75 °C, the hot-spot temperature increased to 150−180 °C. In this case, the difference between the hot-spot and module temperatures increased from 30−50 °C to 70−100 °C. This could be related to dependence of reverse characteristics to temperature change [13,33,35].

Figure 7a shows the thermography of the PERC − Full-cell module when a partially shaded cell is connected in series with 9 cells (bottom) and 19 cells (top). The only difference, other than the fact that they are different cells, is that they have different string lengths. Both cells selected according to IEC 61215-2:2021 have the lowest shunt and the same size shadow mask. As shown in Figure 7b, there is around a 10 °C difference between the hot-spot temperatures. The main reason is that more cells in a string produce a higher negative reverse voltage, which causes the charge carriers to collide with atoms at a higher rate, generating more heat and raising the temperature. There is a strong relation between string length and hot-spot temperature [36]. In PV systems that are expected to be exposed to repeated partial shading, PV modules with shorter strings will improve reliability to avoid potentially dangerous hot-spot temperatures.

Comparing the standard and shortened procedures, similar hot-spot temperatures were obtained for the HS tests performed at 55 °C and 75 °C for all module types. In short, we can conclude that similar hot-spot temperatures obtained in the HS test performed under the worst-case condition (according to the IEC standard) were achieved by following the shortened procedure (less than 5 °C average difference). Although there is a slight temperature difference between the hot-spots that occurred by following the different procedures in some tests, the difference is insignificant. However, it should be noted that the results of the shortened procedure are not generalizable because a total of 7 modules only and 4 module technologies may not

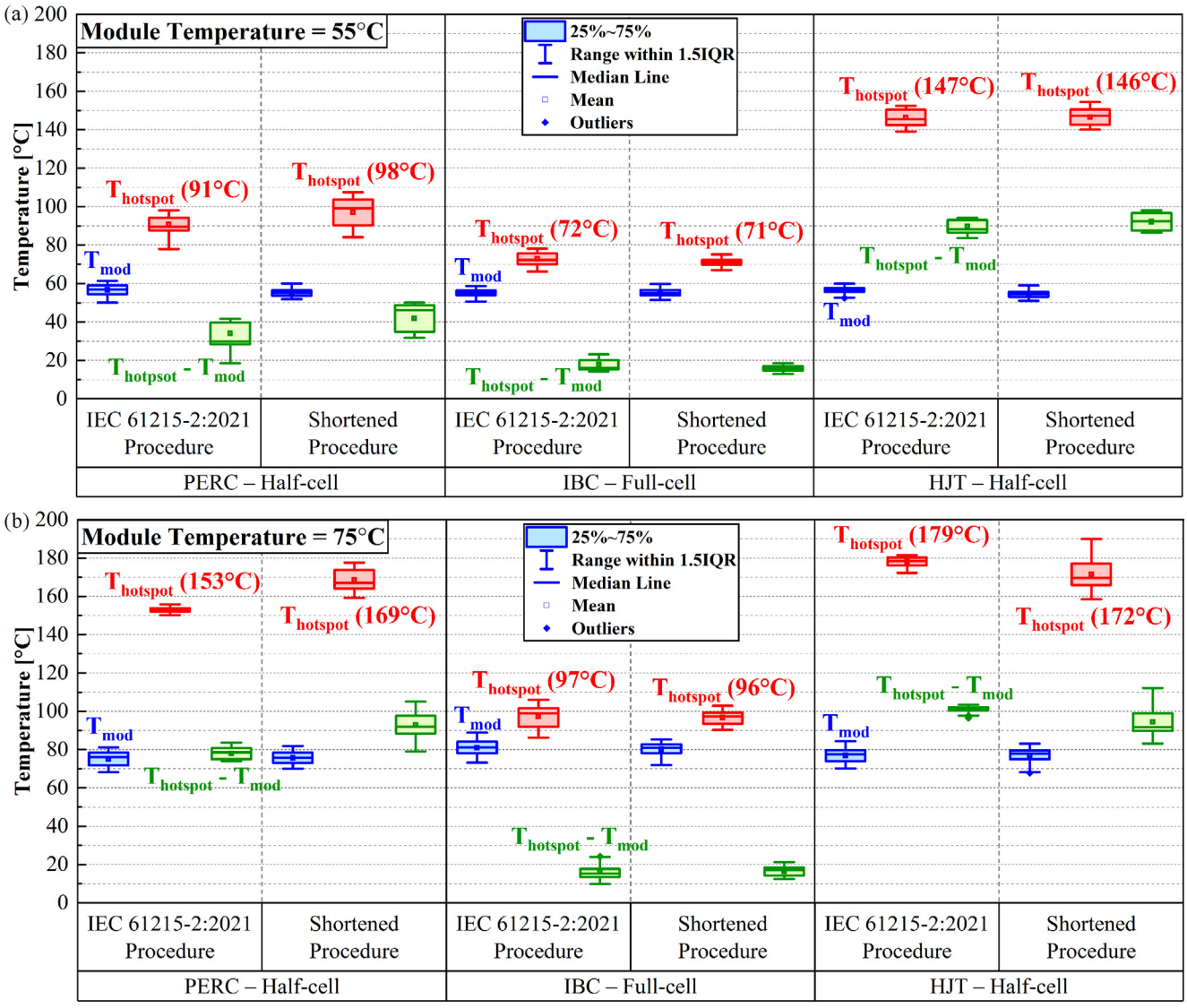

Fig. 6. Module and hot-spot temperatures of PERC – Half-cell, IBC – Full-cell and HJT – Half-cell modules from indoor HS tests at (a) 55 °C and (b) 75 °C module temperature by following IEC 61215-2:2021 and shortened procedures. The error lines reflect the fact that the HS test was performed on multiple cells.

be statistically significant for a generalization. Therefore, these results should be validated with additional experimental work.

3.1.4 Control tests

After the indoor HS test, no visual modification nor changes in electrical performance or insulation were observed with the exception of one single module. Only in the EL of the HJT – Half-cell module, tested at a module temperature of 75 °C, some darkening was observed in the hot-spot parts of the cells that were exposed to partial shading (Fig. 8b). Darkening occurred in both the standard and shortened procedures (Figs. 8b and 8c). With an extended test duration (5 h + 5 h), the darker area and darkening increased even more (Fig. 8d). However, no effect of the darkening on the electrical performance of the module has yet been observed.

The technical specification IEC TS 60904-13:2018 [37] for electroluminescence imaging states that high currents (e.g. I_{sc}) can saturate leakage paths associated with shunts, making cells in a module appear bright except at shunt locations. When current is reduced (e.g. 0.1 × I_{sc}), unsaturated shunt paths may reduce minority carrier density and overall cell EL. In this work, we also performed EL at 0.1 × I_{sc} for all modules. We performed simple image processing to analyse the change in brightness of shaded (1a, 2a, 3a in red) and unshaded (1b, 2b, 3b in blue) cells of the HJT – Full-cell module tested at 75 °C module temperature (Fig. 9). The normalized brightness of the

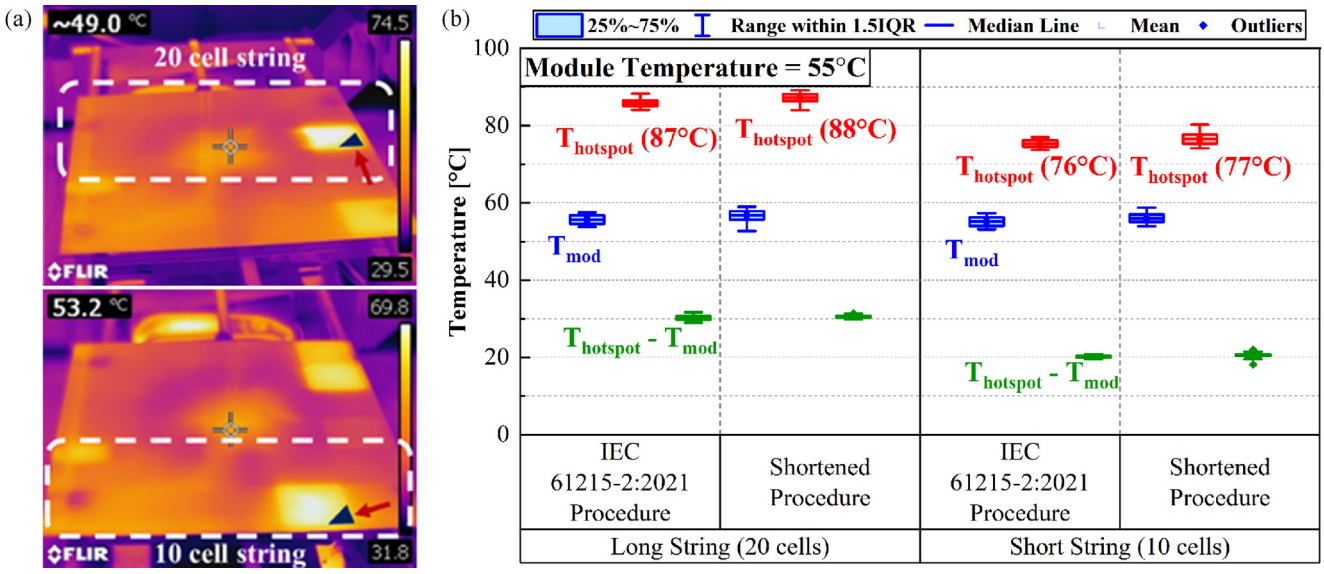

Fig. 7. (a) Thermography images of PERC – Full-cell module while two of its cells (from long and short strings separately) were under the standard HS test. (b) Module and hot-spot temperatures of PERC – Full-cell module from HS tests at 55 °C module temperature by following IEC 61215-2:2021 and shortened procedures. The error lines are due to the fact that the HS test was performed on multiple cells.

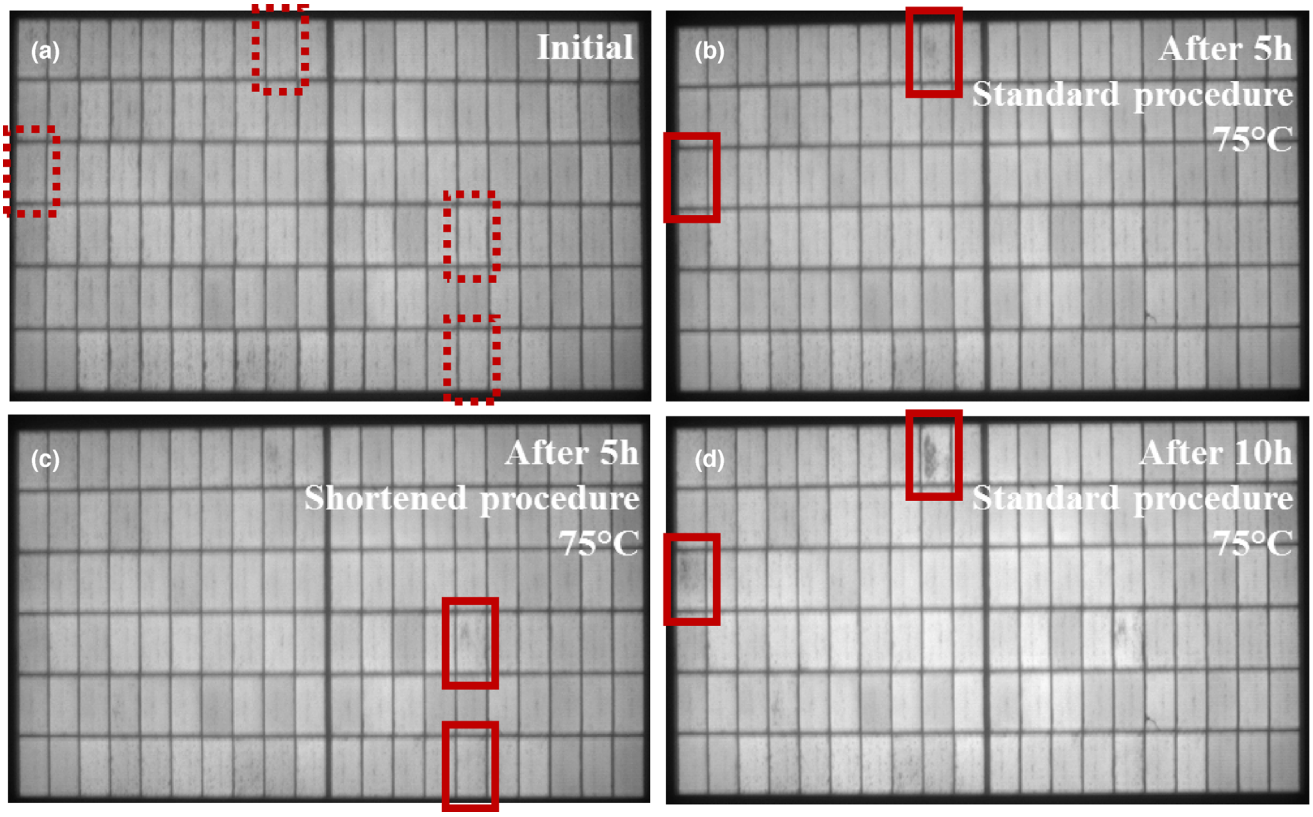

Fig. 8. EL (at I_{sc}) images of HJT – Full-cell module (a) before, (b) after 5 h of standard HS test, (c) after 5 h of shortened HS test and (d) after in total 10 h of standard HS test (same cells as in the first 5 h). The cells to be tested are indicated by the red dotted rectangles. The tested cells are indicated by the red rectangles.

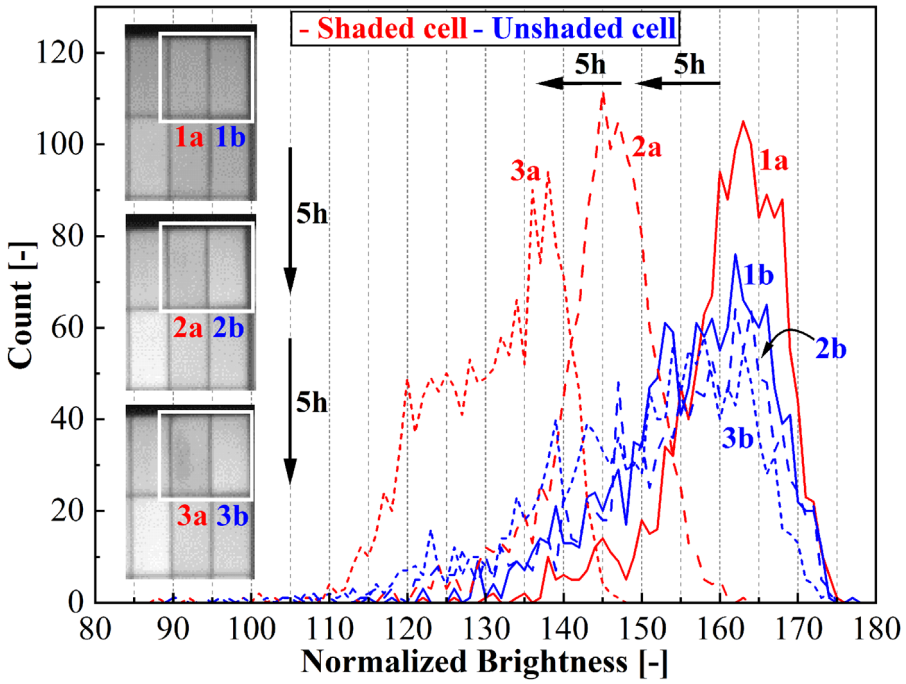

Fig. 9. Histogram of normalized brightness of two cells; shaded (1a, 2a, 3a in red) and unshaded (1b, 2b, 3b in blue) before, after 5 h and after 10 h of the HS testing at 75 °C module temperature of the HJT − Full-cell module. The normalized brightness range is from 0 (black) to 255 (white). EL images taken at 0.1 × I_{sc}.

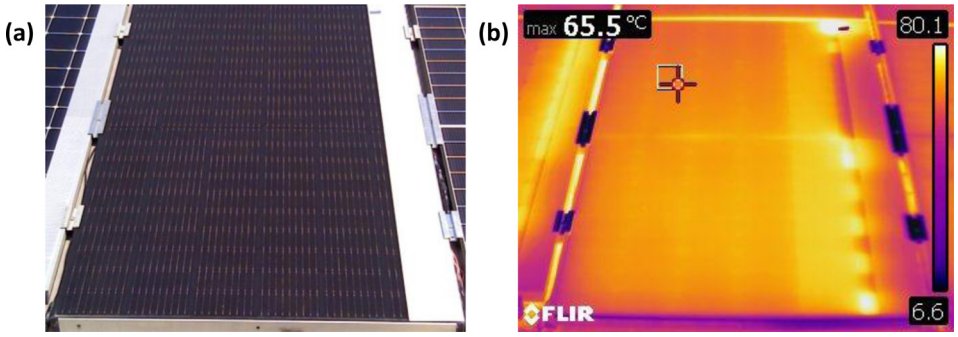

Fig. 10. (a) Digital and (b) thermography images of the PERC − Half-cell module with a shadow mask recorded on a clear-sky day in August 2022.

cells was computed from the EL images (at 0.1 × I_{sc}) taken at initial, after 5 h and after 10 h. Figure 9 illustrates that the maximum and the range of the normalized intensity of the unshaded cell remained relatively constant (in blue), while for the shaded cell, the maximum normalized intensity decreased and the range of intensity increased (in red).

3.2 Outdoor accelerated-ageing tests

3.2.1 Hot-spot temperatures (outdoor)

Figure 10 shows the PERC − Half-cell module with a shadow mask for the BIPV-insulated configuration from the test stand installed on the roof of SUPSI, along with an infrared image identifying the hot-spot locations.

Figures 11a–11d show a typical temperature profile of a clear sky summer day for all four module technologies. The operating module temperature of the BIPV modules reaches higher temperatures in the range of 65 °C to 80 °C compared to open-rack mounted modules. The hot-spot temperatures of the modules vary significantly based on the reverse bias characteristics of the cells, such as the breakdown voltage (IBC − Full-cell module), and the string length. As shown in Figures 11a and 11b, the temperatures reached by the cells in reverse bias can approach 130−140 °C, which is dangerously close to 150 °C. In this case, deterioration of the material or discolouration of the encapsulation is possible, leading to aggravation of the conditions [29,38]. It is important to note that thermal cycling and stressing the diodes (junction box temperature

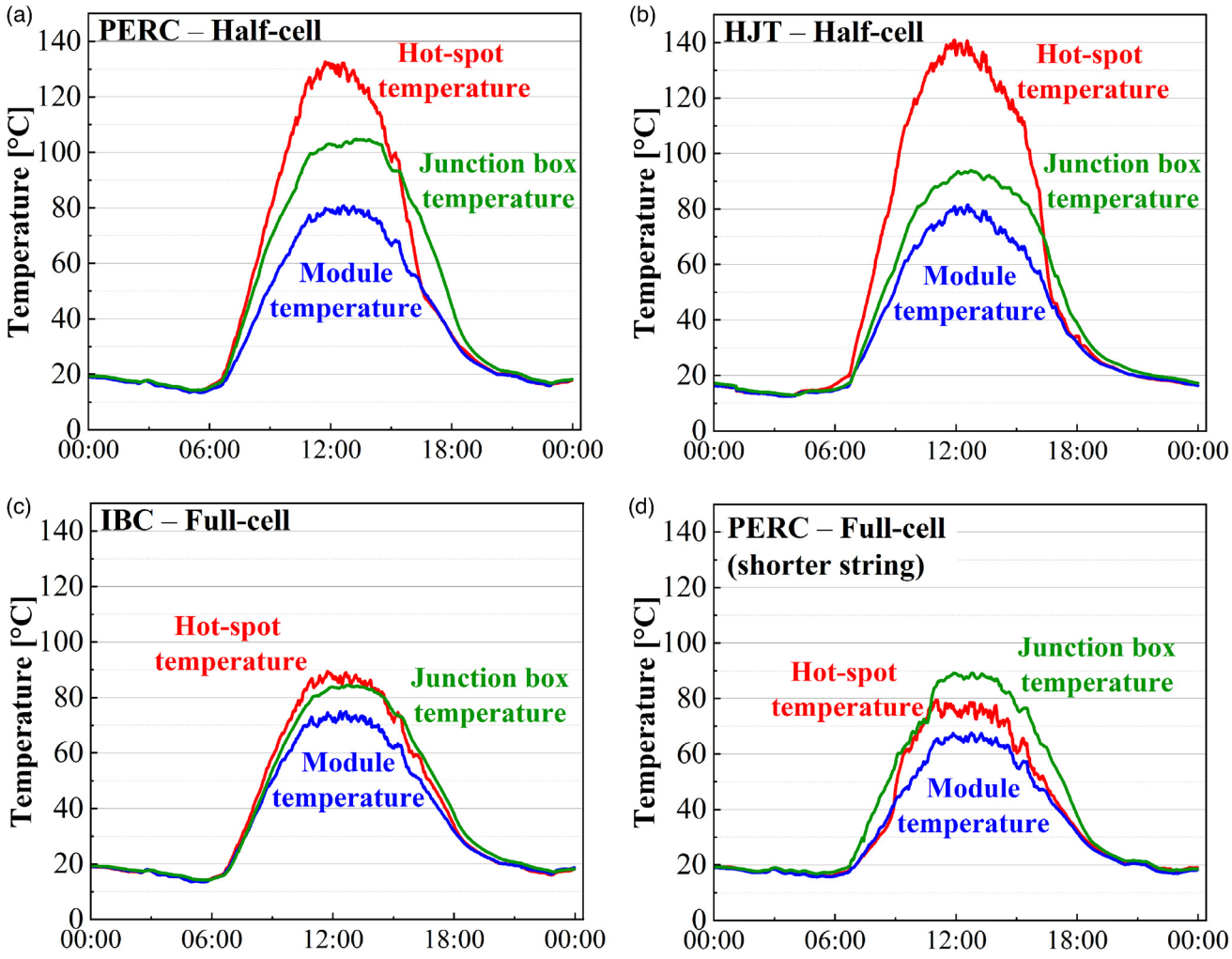

Fig. 11. Daily temperature profiles of the (a) PERC – Half-cell, (b) HJT – Half-cell, (c) IBC – Full-cell and (d) PERC – Full-cell modules with a shadow mask on a clear-sky day in August 2022.

reaches over 100 °C) for prolonged exposure can result in accelerated degradation [39]. In the event of an open-circuit failure in the diode, the cells will no longer be protected from reverse biasing, and the power dissipation will increase significantly, potentially leading to safety concerns. Furthermore, given that the shaded strings are in parallel and both are operating under short-circuit conditions due to the activated BPD, there is the formation of multiple hotspots. In the case of the partially shaded PERC – Full-cell module, there are only 10 cells connected to the BPD, resulting in a hot-spot temperature that is approximately maximum 13 °C higher than the module temperature (Fig. 11d). The IBC module only has a maximum 20 °C difference between its hot-spot and module temperature due to the better reverse bias characteristics of the IBC cell. Figure 11 shows also the junction box temperature. Since the I_{sc} of the modules are similar, and they are all mounted in the same orientation, the currents flowing through the BPDs are approximately equal. Because the BPDs were active (current flowing), the junction box temperatures were at most 10 °C to 20 °C higher than the module temperatures. However, due to the differences in junction box designs and heat transfer, there are slight variations in the junction box temperatures. Without an active BPD (no current flowing), the junction box temperature would be similar or equal to the module temperature.

Figure 12 gives a summary of the measured temperatures over the full testing period. It displays the 98th percentile (T_{98}, 175.2 h per year) and maximum (T_{max}) temperatures of the module, hot-spot, junction box, as well as the difference between hot-spot and module temperatures for all module technologies included in this study. These values were determined using only one year of outdoor monitoring data. The temperatures of the unshaded and shaded modules are similar, indicating that the shadow masks did not significantly impact the operating temperature of the shaded modules (excluding the shaded string).

The highest hot-spot temperature was reached by the HJT module, with a value of 156.5 °C, followed by the PERC – Half-cell module, which recorded a temperature of

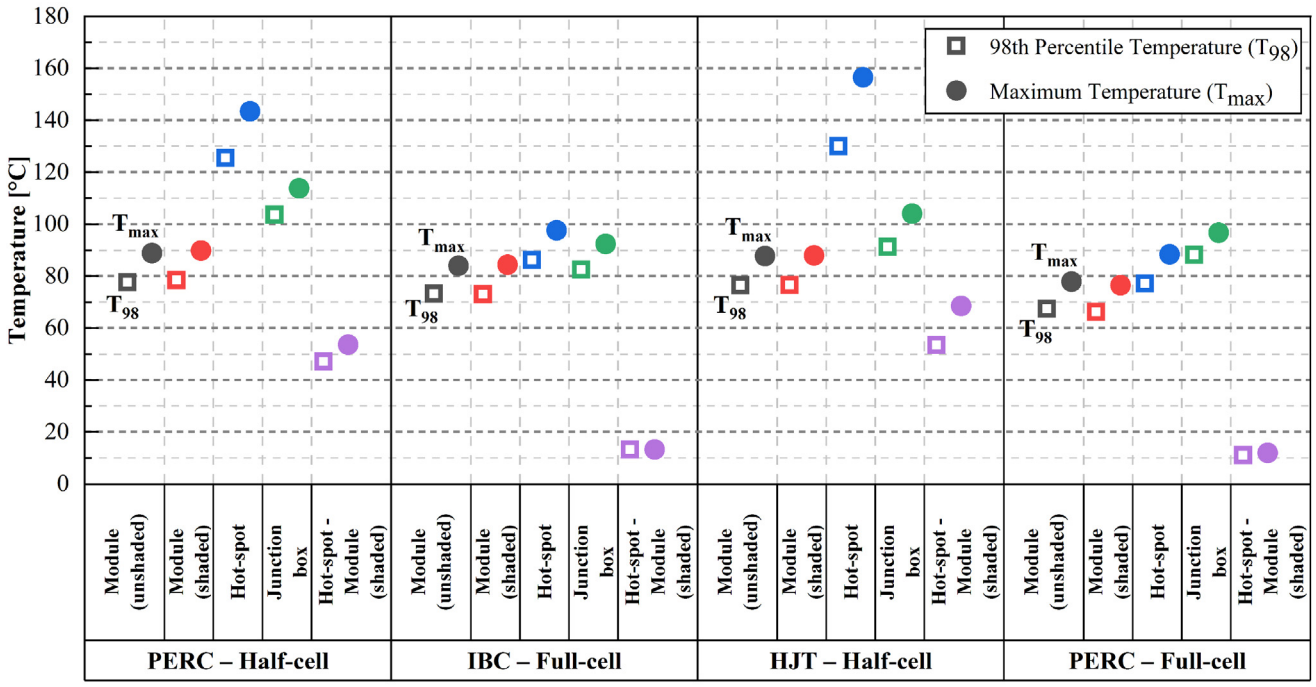

Fig. 12. The 98th percentile (T_{98}) and maximum (T_{max}) values of unshaded module (black), shaded module (red), hot-spot (blue) and junction box (green) temperatures for PERC − Half-cell, IBC − Full-cell, HJT − Half-cell and PERC − Full-cell modules from one-year of outdoor monitoring in BIPV configurations. The difference between hot-spot and mdouel temeprature are shown as well (purple).

143.4 °C. The PERC − Half-cell and HJT − Half-cell modules had the highest T_{98} of hot-spot, at 125.5 °C and 130 °C, respectively.

For the PERC − Full-cell module, the shadow mask was located on the shorter string. As a consequence of the smaller number of cells in the shorter string, the worst-performing cell operated at less negative reverse voltages. This led to a decrease in heat dissipation, reaching a maximum of 88.4 °C, which is significantly lower than that of longer strings. Additionally, there was only a small difference between the hot-spot and module temperatures in this module, at approximately 12 °C. Furthermore, due to the reverse characteristics of the IBC cell, the hot-spot temperature of the IBC module was much lower (maximum 97.6 °C) than the PERC − Half-cell and HJT − Half-cell modules.

3.2.2 Control tests

After 13 months of outdoor monitoring, the IV measurements performed at STC showed a decrease in the performance of both unshaded and shaded modules. However, no performance changes attributable to the shadow masks were detected. As shown in [40], a module's performance can undergo significant changes in the early years due to various degradation modes, which then stabilize. As the suspected degradation modes in this study (i.e. light- and elevated-temperature-induced degradation (LeTID) and/or ultraviolet (UV) radiation-induced degradation [41,42]) are unrelated to shadow masks, this will be the focus of a future study comparing the performance of the same module technologies in open-rack and heat blanket (outdoor accelerated-ageing) configurations in addition to the modules in this study.

The formation of shunt faults at the hot-spot position in the PERC − and HJT − Half-cell modules has not resulted in any significant changes in electrical performance compared to unshaded modules (Figs. 13a and 13c). Moreover, since these modules have two parallel strings connected to an activated BPD, hot-spot formation was detected in both strings simultaneously. This led to a second shunt fault in the HJT module due to the concentration of the second hot-spot in a single area. In contrast, the worst performing cells in the IBC full-cell and PERC full-cell modules did not operate at very high negative voltages in reverse bias due to their lower breakdown voltage and shorter string length, resulting in lower hot-spot temperatures and no shunt faults (Figs. 13b and 13d). All modules exhibited multiple issues in their EL images, such as finger interruption and increasing cell mismatch compared to their initial EL images. These issues are also present in the EL images of the unshaded modules and will be the subject of a future study, as mentioned previously.

Figure 14 depicts visible changes in the encapsulant and backsheet of the PERC-Half-cell module, with accelerated degradation due to high hot-spot temperatures reaching a maximum of 143.4 °C. The presence of irradiation and high temperature can accelerate the UV-induced photo-thermal degradation of polymers [43], leading to accelerated

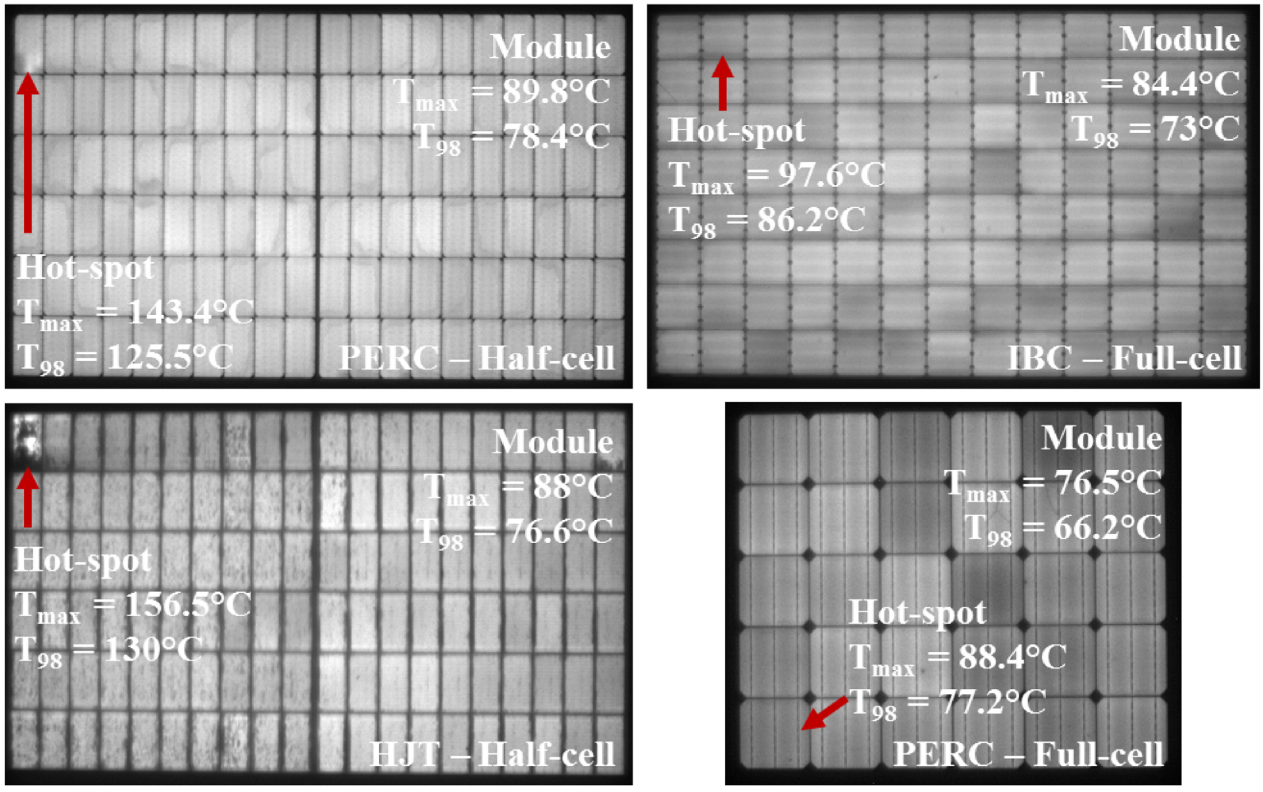

Fig. 13. EL images of the (a) PERC − Half-cell, (b) IBC − Full-cell, (c) HJT − Half-cell and (d) PERC − Full-cell modules after 13 months of outdoor exposure with a shadow mask. The locations of the hot-spots are indicated by red arrows for each module together with the 98th percentile and maximum temperatures of the hot-spots.

discoloration. Photobleaching, a competing process to EVA discoloration in the presence of oxygen penetrating through the backsheet [44], creates a ring without discolouring chromophore species around the solar cell's edge (Fig. 14a). Multiple symmetrical rings can be observed, depending on oxygen diffusion and degradation product mode [45].

4 Discussion

To confirm the accuracy of the HS test in terms of temperature, the hot-spot temperatures obtained through the HS test were compared to the temperatures obtained from outdoor tests utilizing shadow masks. It is expected that the HS test produce higher temperatures due to the fact that the HS test is conducted under the worst-case conditions, whereas the outdoor test aims to simulate a more realistic scenario. In the HS test, a cell is partially shaded (opaque), while in the outdoor test, the long edge is shaded (36% transparent). In addition, the HS test is carried out in the short-circuit condition, while the outdoor test is carried out in the maximum power point condition. With regard to the duration, the outdoor test is a form of accelerated-ageing due to the shadow mask. However, it should be noted that the maximum duration of the HS test is 5 h. As such, the HS test can be only few days of the outdoor test, depending on the weather conditions.

The range of the T_{98} for the BIPV-insulated modules is between 70 °C and 80 °C (Fig. 15). According to IEC TS 63126:2020, this requires Level 1 test conditions for the selected safety and reliability tests including the HS test. IEC TS 63126:2020 suggests to perform the HS test at a module temperature of 60±10 °C instead of the standard 55±15 °C (Tab. 3). We performed the HS test at 55 °C, but at the time of this test the average temperature of the PERC − Half-cell module was 57 °C, which is very close to 60 °C (Fig. 15). This HS test on the PERC − Half-cell module achieved an average hot-spot temperature of 92 °C, while the hot-spot of the module that needs to be tested at Level 1 according to IEC TS 63126:2020 has reached a maximum of 144 °C in the outdoor conditions (Fig. 15). When the HS test was performed at the module temperature recommended by IEC TS 63126:2020, even T_{98} of the hot-spot (126 °C) of this module could not be reached. However, when we performed the HS test at a module temperature of 75 °C, the average hot-spot temperature (152 °C) slightly higher than the maximum hot-spot temperature (144 °C) obtained in the 13-month outdoor monitoring was obtained by the HS test (Fig. 15). As shown in Figure 15, a similar situation occurred in other modules.

The hot-spot temperatures obtained from the indoor HS tests at 75 °C are neither too high nor too low compared to the hot-spot temperatures observed in the field (Fig. 15). Considering that the HS test is designed to test the worst-case

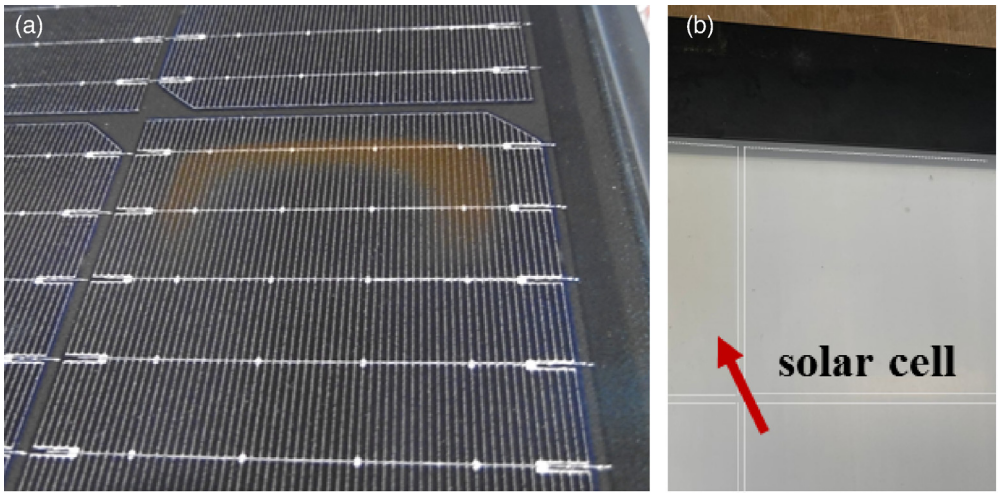

Fig. 14. Discoloration of (a) encapsulant and (b) backsheet of the PERC − Half-cell module after 13 months of operation with a shadow mask. The discoloration of the backsheet is indicated by a red arrow. Dashed lines indicate the edges of the solar cells.

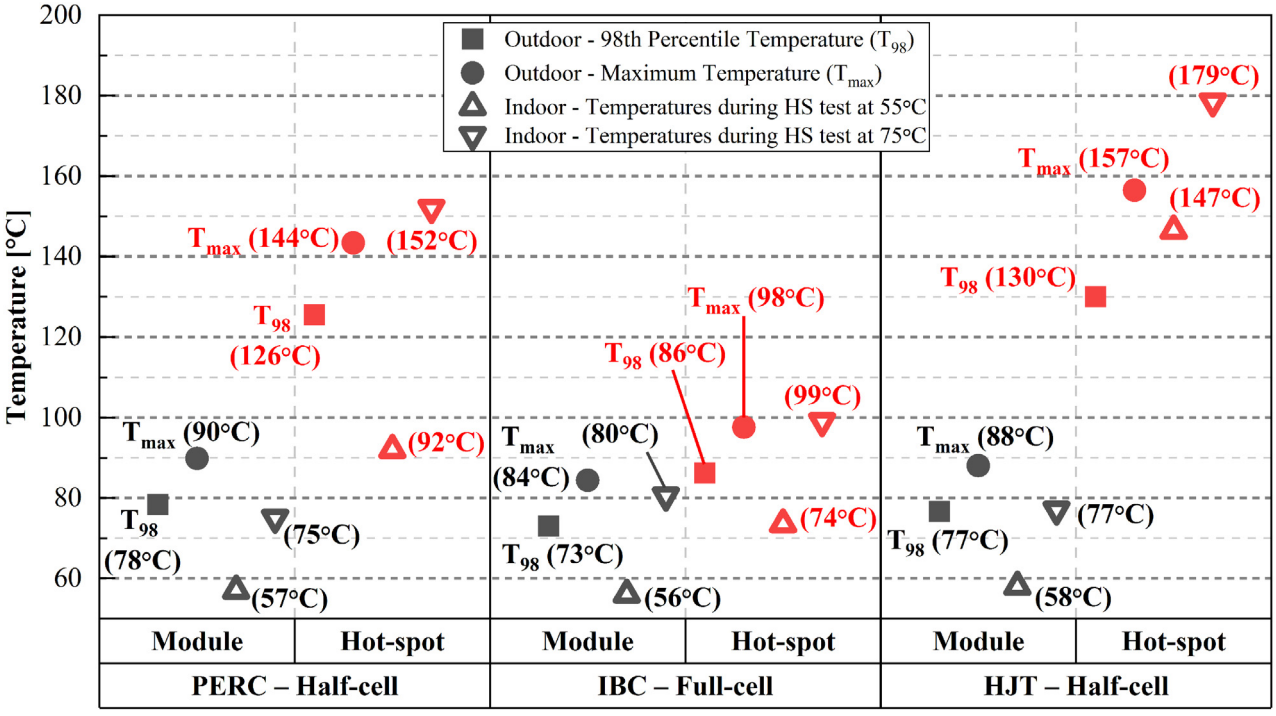

Fig. 15. The 98th percentile (T_{98}) and maximum (T_{max}) temperatures of shaded module (black), hot-spot (red) for PERC − Half-cell, IBC − Full-cell and HJT − Half-cell modules from one-year of outdoor monitoring in BIPV-Insulated configuration (filled symbols). The module and hot-spot temperatures during the indoor HS tests at 55 °C and 75 °C (unfilled symbols).

conditions, it would be more realistic to perform this test at a module temperature of 75 °C and 85 °C for Level 1 (70 °C < T_{98} ≤ 80 °C) and Level 2 (80 °C < T_{98} ≤ 90 °C) at IEC TS 63126:2020, respectively. Recommendations for adapting the technical specification IEC TS 63126:2020 are given in Table 3.

Beside the temperatures at which the test is carried out, the duration of the test is discussed here. Table 4 shows the simulated total duration of a partial shadow per year under certain assumptions for Mendrisio, Switzerland. This simulation assumed diode activation, hot-spot formation, and a stable hot-spot location. For these reasons, although the probability of residential PV systems experiencing more than 1 h of partial shade per day is high if the above conditions are not met, in this simulation, we have assumed that the daily duration of partial shade is a maximum of 30 min. The simulated annual duration of partial shade (with hot-spot) is 11, 33, and 66 h per year for low, medium, and high shading intensities, respectively. The

Table 3. The recommendations from this study for HS test conditions in IEC TS 63126:2020.

Hot-spot endurance test	Standard (IEC 61215:2021)	Level 1 (70 °C < T_{98} ≤ 80 °C)	Level 2 (80 °C < T_{98} ≤ 90 °C)
IEC TS 63126:2020*	55±15 °C	60±10 °C	70±10 °C
Proposal of this study	55±15 °C	75±10 °C	85±10 °C

*When IEC TS 63126:2020 was published, still IEC 61215-2:2016 was in action and module temperature of the HS test was 50±10 °C.

Table 4. Simulation of the annual duration of partial shade for different shadow intensities. Diode activation, hot-spot formation, and a stable hot-spot location were assumed.

Shadow intensity	Duration of daily partial shade	Percentage of clear sky days per year (Mendrisio, Switzerland)	Annual duration of partial shadow
Low intensity	5 min	36%*	11 h/year
Medium intensity	15 min		33 h/year
High intensity	30 min		66 h/year

*Calculated from the monitored global horizontal and diffused irradiance.

maximum possible duration of the HS test (5 h) does not cover one year of any of these shading intensities. The standard duration of the HS test simulates a maximum of 2.5 min of partial shade per day for only one year for the simulated location. It should be noted that the HS test creates a hot-spot at a temperature higher than the most realistic conditions (assuming no failed diode), thus accelerating this test using higher thermal stress. Performing the HS test in outdoor may be useful to extend the duration of the test, but in this case, the control over the module temperature and irradiation will be more difficult.

5 Summary and conclusion

In residential PV systems, PV modules are commonly exposed to partial shading from various sources, such as chimneys or other buildings. This shading can potentially result in localized hot-spots on the module, which, if the temperature and frequency of these hot-spots are high enough, can compromise the reliability and safety of the PV module. To evaluate the materials' ability to withstand these extreme conditions, the hot-spot endurance test, as per the IEC 61215-2:2021 standard, is utilized. In residential systems, the type of installation (building attached PV or building integrated PV) and weather conditions can cause PV modules to operate at higher temperatures than those in open fields. Therefore, some modifications to the test conditions of selected reliability tests, including the hot-spot endurance test, are recommended in IEC TS 63126. In this study, the hot-spot endurance tests were conducted under the standard (at 55 °C module temperature) and most severe test conditions specified in IEC TS 63126:2020 (at 75 °C module temperature), and outdoor accelerated-ageing tests were carried out using shadow masks.

Based on the reverse characteristics of the IBC cell, including its diode functionality, uniform heating, and lower breakdown voltage, the IBC module exhibited a more favorable performance under partial shade compared to other module technologies (i.e. PERC and HJT). Specifically, the hot-spot temperature remained a maximum of 25 °C higher than the module temperature, and it was significantly lower than that of other module technologies, averaging 60 °C less. In addition, this study indicates that connecting a cell operating in reverse bias due to partial shading to a shorter string can result in a decrease in hot-spot temperature, as it operates at lower reverse voltages. By reducing the number of cells in a string from 20 to 10, 10 °C lower hot-spot temperatures were achieved under the same conditions in the indoor HS test. As shading is a common occurrence in residential PV systems, shorter string lengths or shadow-tolerant cell technologies can improve the reliability and long-term performance of a system.

A shortened procedure was performed that could reduce the cell selection (Step 1) and worst-case shading determination (Step 2) steps of the HS test by at least 120 min in a conventional 120 half-cell module. It has been observed that the shortened procedure for the hot-spot endurance test, when utilized, produced results that are comparable to those obtained through implementation of the standard test (less than 5 °C average difference). However, only 7 modules and 4 module types were tested during these evaluations. To validate the effectiveness of the shortened process, a larger sample size comprising additional module types must be tested. Most importantly, the shortened procedure is appropriate only if the reverse bias behaviour of the cells can be assumed to be identical.

Lastly, this study found that the hot-spot temperature of the modules, which should be tested under Level 1 conditions of the hot-spot endurance test as per IEC TS 63126:2020, is significantly higher in the outdoor conditions than the

temperatures achieved during the hot-spot endurance tests at Level 1 conditions (average module temperature of 57 °C). It is recommended that more realistic hot-spot temperatures can be achieved by conducting the hot-spot endurance test at a module temperature of 75 °C, which exceeds the recommended test temperatures in IEC TS 63126:2020 for HS testing at Level 1 conditions. As a result, it is suggested that the module temperatures for both Level 1 and Level 2 conditions in IEC TS 63126:2020 be increased by 15 °C to enhance the accuracy of the HS test.

Acknowledgments

The project called "Reliability of PV Systems integrated into the built environment" (REBIPV) is supported by the Swiss National Science Foundation under COST IZCOZ0_182967 and the Swiss Federal Office of Energy. We would like to thank Nicolas Ostinelli, Enrico Burà and Boris Margna for their great help in designing and installing the outdoor test stands. We would also like to thank Moreno Ronchi and Mattia Ceretti for their help with the indoor measurements. Finally, we would like to thank Giovanni Bellenda for helpful discussions on standard tests and other possibilities.

Funding

The project called "Reliability of PV Systems integrated into the built environment" (REBIPV) is funded by the Swiss National Science Foundation under COST IZCOZ0_182967 and the Swiss Federal Office of Energy.

Conflicts of interest

All authors declare that they have no conflicts of interest.

Data availability statement

Data associated with this article will not be disclosed.

Author contribution statement

The authors confirm contribution to the paper as follows: study conception, design: E. Özkalay; data collection: E. Özkalay, F. Valoti; analysis and interpretation of results: E. Özkalay; draft manuscript preparation: E. Özkalay, A. Virtuani; funding acquisition: M. Caccivio, G. Friesen, C. Ballif; project management: A. Virtuani, G. Friesen, C. Ballif. All authors reviewed the results, participated in the review and revision of the manuscript, and approved the final version of the manuscript.

References

1. A. Fairbrother, H. Quest, E. Özkalay, P. Wälchi, G. Friesen, C. Ballif, Long-term performance and shade detection in building integrated photovoltaic systems, Solar RRL **6**, 2100583 (2022)
2. M. Caccivio, E. Özkalay, D. Chianese, Photovoltaïque intégré au bâti et ombrage - Défis et solutions, bulletin.ch, September 2022
3. E. Özkalay, G. Friesen, M. Caccivio, P. Bonomo, A. Fairbrother, C. Ballif, A. Virtuani, Operating temperatures and diurnal temperature variations of modules installed in open-rack and typical BIPV configurations, IEEE J. Photovoltaic **12**, 133 (2022)
4. D. Jordan, S. Kurts, K. VanSant, J. Newmiller, Compendium of photovoltaic degradation rates, Progr. Photovolt. **24**, 978 (2016)
5. H. Hu, W. Gambogi, K.R. Choudhury, L. Garreau-Iles, T. Felder, S. MacMaster, O. Fu, T.-J. Trout, Field analysis and degradation of modules and components in distributed PV applications, in *35th European Photovoltaic Solar Energy Conference and Exhibition*, 2018
6. IEC, IEC 61215-2:2021 Terrestrial photovoltaic (PV) modules - design qualification and type approval - Part 2: Test procedures, International Electrotechnical Commission, 2021
7. IEC, IEC 61730-2:2023 Photovoltaic (PV) module safety qualification - Part 2: requirements for testing, International Electrotechnical Commission, 2023
8. IEC, IEC TS 63126:2020 ED1 Guidelines for qualifying PV modules, components and materials for operation at high temperatures, International Electrotechnical Commission, 2020
9. IEA Task 13, Service Life Estimation for Photovoltaic Modules, International Energy Agency, 2021
10. R. Witteck, M. Siebert, S. Blankemeyer, H. Schulte-Huxel, M. Köntges, Three bypass diodes architecture at the limit, IEEE J. Photovoltaics **10**, 1828 (2020)
11. M. Alonso-García, J. Ruiz, F. Chenlo, Experimental study of mismatch and shading effects in the I–V characteristic of a photovoltaic module, Solar Energy Mater. Solar Cells **90**, 329 (2006)
12. K. Kim, P. Krein, Photovoltaic hot spot analysis for cells with various reverse-bias characteristics through electrical and thermal simulation, in *2013 IEEE 14th Workshop on Control and Modeling for Power Electronics (COMPEL)*, Salt Lake City, 2013
13. O. Breitenstein, J. Bauer, K. Bothe, W. Kwapil, D. Lausch, U. Rau, J. Schmidt, M. Schneemann, M. Schubert, J. Wagner, W. Warta, Understanding junction breakdown in multicrystalline solar cells, J. Appl. Phys. **109**, 071101 (2011)
14. J. Bauer, J.-M. Wagner, A. Lotnyk, H. Blumtritt, N. Zakharov, O. Breitenstein, Physical mechanisms of electrical breakdown in silicon solar cells, 2009
15. K. Al Abdullah, F. Al Alloush, A. Jaafar, C. Salame, Study of the effects related to the electric reverse stress study of the effects related to the electric reverse stress, Energy Procedia **36**, 104 (2013)
16. Y. Jia, Y. Wang, X. Hu, J. Xu, G. Weng, X. Luo, S. Chen, Z. Zhu, H. Akiyama, Diagnosing breakdown mechanisms in monocrystalline silicon solar cells via electroluminescence imaging, Solar Energy **225**, 463 (2021)
17. K.A. Kim, P.T. Krein, Hot spotting and second breakdown effects on reverse I-V characteristics for mono-crystalline Si photovoltaics, in *IEEE Energy Conversion Congress and Exposition,* Denver, 2013
18. W. Herrman, M. Adrian, W. Wiesner, Operational behaviour of commercial solar cells under reverse biased conditions, in *2nd WCPEC*, Vienna, 1998

19. W. Hermann, et al., Effective hot-spot protection of PV modules - characteristics of crystalline silicon cells and consequences for cell production, in *European Photovoltaic Solar Energy Conference and Exhibition (EU PVSEC)*, 2001
20. F. Fertig, S. Rein, M. Schubert, W. Warta, Impact of junction breakdown in multi-crystalline silicon solar cells on hot spot formation and module performance, in *26th European PV Solar Energy Conference and Exhibition*, Hamburg, 2011
21. J. Appelbaum, A. Chait, D. Thompson, Parameter estimation and screening of solar cells, Progr. Photovolt. Res. Appl. **1**, 93 (1993)
22. J. Wohlgemuth, W. Herrmann, Hot spot tests for crystalline silicon modules, in *Proceedings IEEE Photovoltaic Specialists Conference*, 2005
23. J. Hudson, L. Vasilyev, J. Schmidt, G. Horner, Economic impacts and approaches to address hot-spot defects in photovoltaic devices, in *Proceedings 35th IEEE Photovoltaic Specialists Conference* (IOEEE, 2010)
24. R. Vieira, F. de Araújo, M. Dhimish, M. Guerra, A comprehensive review on bypass diode application on photovoltaic modules, Energies **13**, 2472 (2020)
25. H. Hanifi, J. Schneider, J. Bagdahn, Reduced shading effect on half-cell modules – measurement and simulation, in *31st European Photovoltaic Solar Energy Conference and Exhibition*, 2015
26. N. Klasen, D. Weisser, T. Rößler, D.H. Neuhaus, A. Kraft, Performance of shingled solar modules under partial shading, Prog. Photovolt. Res. Appl. **30**, 325 (2022)
27. C.D. Jordan, T.J. Silverman, J.M. Wohlgemuth, S.R. Kurtz, K.T. VanSant, Photovoltaic failure and degradation modes, Progr. Photovolt. Res. Appl. **25**, 318 (2017)
28. A. Brooks, D. Cormode, A. Cronin, E. Kam-Lum, PV system power loss and module damage due to partial shade and bypass diode failure depend on cell behavior in reverse bias, in *IEEE 42nd Photovoltaic Specialist Conference (PVSC)*, New Orleans, 2015
29. W. Herrmann, W. Wiesner, W. Vaassen, Hot spot investigations on PV modules-new concepts for a test standard and consequences for module design with respect to bypass diodes, in *26th IEEE PVSC*, 1997
30. I. Geisemeyer, F. Fertig, W. Warta, S. Rein, M. Schubert, Prediction of silicon PV module temperature for hot spots and worst case partial shading situations using spatially resolved lock-in thermography, Sol. Energy Mater. Sol. Cells **120**, 259 (2014)
31. D.M. Kempe, D. Holsapple, K. Whitfield, N. Shiradkar, Standards development for modules in high temperature micro-environments, Progr. Photovolt. Res. Appl. **29**, 445 (2021)
32. M. Kottek, J. Grieser, C. Beck, B. Rudolf, F. Rubel, World map of the Köppen-Geiger climate classification, Meteorol. Zeitsch. **15**, 259 (2006)
33. H. Chu, L. Koduvelikulathu, V. Mihailetchi, G. Galbiati, A. Halm, R. Kopecek, Soft breakdown behavior of interdigitated-back-contact silicon solar cells, in *5th International Conference on Silicon Photovoltaics*, 2015
34. R. Müller, C. Reichel, J. Schrof, M. Padilla, M. Selinger, I. Geisemeyer, J. Benick, M. Hermle, Analysisof n-type IBC solar cells with diffused boron emitter locally blocked by implanted phosphorus, Sol. Energy Mater. Sol. Cells **142**, 54 (2015)
35. A. Dhass, P. Lakshmi, E. Natarajan, Investigation of performance parameters of different photovoltaic cell materials using the lambert-w function, Energy Procedia **90**, 566 (2016)
36. Q. Zhang, L. Qun, Temperature and reverse voltage across a partially shaded Si PV cell, in *38th IEEE Photovoltaic Specialists Conference*, Austin, 2012
37. IEC, IEC TS 60904-13:2018 Photovoltaic devices - Part 13: Electroluminescence of photovoltaic modules, International Electrotechnical Commission, 2018
38. S. Wendlandt, A. Drobisch, T. Buseth, S. Krauter, P. Grunow, Hotspot risk analysis on silicon cell modules, in *26th European Photovoltaic Solar Energy Conference and Exhibition*, 2010
39. Z. Zhang, J. Wohlgemuth, S. Kurtz, Thermal reliability study of bypass diodes in photovoltaic modules, in *Photovoltaic Module Reliability Workshop*, Golden, 2013
40. M. Theristis, J. Stein, C. Deline, D. Jordan, C. Robinson, W. Sekulic, A. Anderberg, D. Colvin, J. Walters, H. Seignur, B. King, Onymous early-life performance degradation analysis of recent photovoltaic module technologies, Progr. Photovoltaics **31**, 149 (2023)
41. J. Karas, I. Repins, K. Berger, B. Kubicek, F. Jiang, D. Zhang, J. Jaubert, A. Cueli, T. Sample, B. Jaeckel, M. Pander, E. Fokuhl, M.Koentopp, F. Kersten, J. Choi, B. Bora, C. Banerjee, S. Wendlandt, T. Erion-Lorico, K. Sauer, J. Tsan, M. Pravettoni, M. Caccivio, G. Bellenda, C. Monokroussos, H. Maaroufi, Results from an international interlaboratory study on light-and elevated temperature-induced degradation in solar modules, Progr. Photovoltaics **30**, 1255 (2022)
42. A. Sinha, J. Qian, S. Moffit, K. Hurst, K. Terwilliger, D. Miller, L. Schelhas, P. Hacke, UV-induced degradation of high-efficiency silicon PV modules with different cell architectures, Progr. Photovoltaics **1**, 36 (2023)
43. A. Czanderna, F. Pern, Encapsulation of PV modules using ethylene vinyl acetate copolymer as a pottant: a critical review, Sol. Energy Mater. Sol. Cells **43**, 101 (1996)
44. F.J. Pern, S.H. Glick, Fluorescence analysis as a diagnostic tool for polymer encapsulation processing and degradation, AIP Conf. Proc. **306**, 573 (1994)
45. IEA Task 13, Review of Failures of Photovoltaic Modules, International Energy Agency, 2014

Cite this article as: Ebrar Özkalay, Flavio Valoti, Mauro Caccivio, Alessandro Virtuani, Gabi Friesen, Christophe Ballif, The effect of partial shading on the reliability of photovoltaic modules in the built-environment, EPJ Photovoltaics **15**, 7 (2024)